

Journal of Visualized Experiments

Fabrication and Characterization of Thickness Mode Piezoelectric Devices for Atomization and Acoustofluidics --Manuscript Draft--

Article Type:	Invited Methods Article - JoVE Produced Video
Manuscript Number:	JoVE61015R2
Full Title:	Fabrication and Characterization of Thickness Mode Piezoelectric Devices for Atomization and Acoustofluidics
Section/Category:	JoVE Engineering
Keywords:	acoustofluidics; lab on a chip; Microfluidics; atomizer; nebulizer; piezoelectricity; ultrasound; acoustics; bioengineering; nonlinear acoustics; physical acoustics; microfabrication
Corresponding Author:	James Friend University of California-San Diego La Jolla, California UNITED STATES
Corresponding Author's Institution:	University of California-San Diego
Corresponding Author E-Mail:	jfriend@eng.ucsd.edu
Order of Authors:	Aditya Vasan William Connacher James Friend
Additional Information:	
Question	Response
Please indicate whether this article will be Standard Access or Open Access.	Standard Access (US\$2,400)
Please indicate the city, state/province, and country where this article will be filmed. Please do not use abbreviations.	La Jolla, CA USA

TITLE:

Fabrication and Characterization of Thickness Mode Piezoelectric Devices for Atomization and Acoustofluidics

AUTHORS AND AFFILIATIONS:

Aditya Vasan¹, William Connacher¹, James Friend¹

¹Medically Advanced Devices Laboratory, Center for Medical Devices, Department of Mechanical and Aerospace Engineering, Jacobs School of Engineering and Department of Surgery, School of Medicine, University of California San Diego, La Jolla, CA, USA

Corresponding Author:

James Friend (jfriend@eng.ucsd.edu)

Email Addresses of Co-Authors:

Aditya Vasan (advasan@eng.ucsd.edu)

William Connacher (wconnacher@eng.ucsd.edu)

KEYWORDS:

acoustofluidics, lithium niobate, atomization, laser doppler vibrometry, high-speed imaging, nebulizer

SUMMARY:

Fabrication of piezoelectric thickness mode transducers via direct current sputtering of plate electrodes on lithium niobate is described. Additionally, reliable operation is achieved with a transducer holder and fluid supply system and characterization is demonstrated via impedance analysis, laser doppler vibrometry, high-speed imaging, and droplet size distribution using laser scattering.

ABSTRACT:

We present a technique to fabricate simple thickness mode piezoelectric devices using lithium niobate (LN). Such devices have been shown to atomize liquid more efficiently, in terms of flow rate per power input, than those that rely on Rayleigh waves and other modes of vibration in LN or lead zirconate titanate (PZT). The complete device is composed of a transducer, a transducer holder, and a fluid supply system. The fundamentals of acoustic liquid atomization are not well known, so techniques to characterize the devices and to study the phenomena are also described. Laser Doppler vibrometry (LDV) provides vibration information essential in comparing acoustic transducers and, in this case, indicates whether a device will perform well in thickness vibration. It can also be used to find the resonance frequency of the device, though this information is obtained more quickly via impedance analysis. Continuous fluid atomization, as an example application, requires careful fluid flow control, and we present such a method with high-speed imaging and droplet size distribution measurements via laser scattering.

INTRODUCTION:

45 Ultrasound atomization has been studied for almost a century and although there are many
46 applications, there are limitations in understanding the underlying physics. The first description
47 of the phenomenon was made by Wood and Loomis in 1927¹, and since then there have been
48 developments in the field for applications ranging from delivering aerosolized pharmaceutical
49 fluids² to fuel injection³. Although the phenomenon works well in these applications, the
50 underlying physics is not well understood^{4,5,6}.

51
52 A key limitation in the field of ultrasonic atomization is the choice of material used, lead
53 zirconate titanate (PZT), a hysteretic material prone to heating⁷ and lead contamination with
54 elemental lead available from the inter-grain boundaries^{8,9}. Grain size and mechanical and
55 electronic properties of grain boundaries also limit the frequency at which PZT can operate¹⁰.
56 By contrast, lithium niobate is both lead-free and exhibits no hysteresis¹¹, and can be used to
57 atomize fluids an order of magnitude more efficiently than commercial atomizers¹². The
58 traditional cut of lithium niobate used for operation in the thickness mode is the 36-degree Y-
59 rotated cut, but the 127.86-degree Y-rotated, X-propagating cut (128YX), typically used for
60 surface acoustic wave generation, has been shown to have a higher surface displacement
61 amplitude in comparison with the 36-degree cut¹³ when operated in resonance and low loss. It
62 has also been shown that thickness mode operation offers an order of magnitude improvement
63 in atomizer efficiency over other modes of vibration¹³, even when using LN.

64
65 The resonance frequency of a piezoelectric device operating in the thickness mode is governed
66 by its thickness t : the wavelength $\lambda = 2t/n$ where $n = 1, 2, \dots$ is the number of anti-nodes. For a
67 500 μm thick substrate, this corresponds to a wavelength of 1 mm for the fundamental mode,
68 which can then be used to calculate the fundamental resonance frequency, $f = v/\lambda$ if the
69 wave speed, v , is known. The speed of sound through the thickness of 128YX LN is
70 approximately 7,000 m/s, and so $f = 7$ MHz. Unlike other forms of vibration, particularly
71 surface-bound modes, it is straightforward to excite higher-order thickness mode harmonics to
72 much higher frequencies, here to 250 MHz or more, though only the odd-numbered modes
73 may be excited by uniform electric fields¹⁴. Consequently, the second harmonic ($n = 2$) near 14
74 MHz cannot be excited, but the third harmonic at 21 MHz ($n = 3$) can. Fabrication of efficient
75 thickness mode devices requires depositing electrodes onto opposing faces of the transducer.
76 We use direct current (DC) sputtering to accomplish this, but electron-beam deposition and
77 other methods could be used. Impedance analysis is useful to characterize the devices,
78 particularly in finding the resonance frequencies and electromechanical coupling at these
79 frequencies. Laser Doppler vibrometry (LDV) is useful to determine the output vibration
80 amplitude and velocity without contact or calibration¹⁵, and, via scanning, the LDV provides the
81 spatial distribution of surface deformation, revealing the mode of vibration associated with a
82 given frequency. Finally, for the purposes of studying atomization and fluid dynamics, high-
83 speed imaging can be employed as a technique to study the development of capillary waves on
84 the surface of a sessile drop^{16,17}. In atomization, like many other acoustofluidic phenomena,
85 small droplets are produced at a rapid rate, over 1 kHz in a given location, too quickly for high-
86 speed cameras to observe with sufficient fidelity and field of view to provide useful information
87 over a sufficiently large droplet sample size. Laser scattering may be used for this purpose,
88 passing the droplets through an expanded laser beam to (Mie) scatter some of the light in

reflection and refraction to produce a characteristic signal that may be used to statistically estimate the droplet size distribution.

It is straightforward to fabricate piezoelectric thickness mode transducers, but the techniques required in device and atomization characterization have not been clearly stated in the literature to date, hampering progress in the discipline. In order for a thickness mode transducer to be effective in an atomization device, it must be mechanically isolated so that its vibration is not damped and it must have a continuous fluid supply with a flow rate equal to the atomization rate so that neither desiccation nor flooding occur. These two practical considerations have not been thoroughly covered in the literature because their solutions are the result of engineering techniques rather than pure scientific novelty, but they are nonetheless critical to studying the phenomenon. We present a transducer holder assembly and a liquid wicking system as solutions. This protocol offers a systematic approach to atomizer fabrication and characterization for facilitating further research in fundamental physics and myriad applications.

PROTOCOL:

1. Thickness mode transducer fabrication via DC sputtering

1.1. Wafer preparation

1.1.1. Place a 100 mm 128YX LN wafer in a clean glass dish of at least 125 mm diameter. Sonicate the wafer in at least 200 mL of acetone for 5 min.

1.1.2. Repeat sonication with isopropyl alcohol and again with deionized water for 5 min each.

1.1.3. Remove visible water from the surface using dry nitrogen.

1.1.4. Completely remove water from the surface by placing the wafer on a hotplate at 100 °C for 5 min. Ensure that there is a sheet of aluminum foil on the hotplate as this helps in dissipation of charge buildup on the wafer.

1.2. Electrode deposition

1.2.1. Place the wafer in the vacuum chamber of the sputter deposition system and pump down the chamber to 5×10^{-6} mTorr. Set the argon pressure to 2.3 mTorr and the rotation speed to 13 rpm.

NOTE: If parameters for the specific instrument being used have been established that result in high quality films, then use those instead.

1.2.2. Deposit 5–10 nm of titanium at 1.2–1.6 A/s.

NOTE: Before beginning this process with the intended wafer, test the deposition rate with the plasma power set to 200 W and depositing for 1 min. Then measure the height of the layer with a profilometer. Do this separately for each metal. Set the power according to this test in order to achieve the stated deposition rate.

1.2.3. Deposit 1 μm of gold at 7–9 A/s.

NOTE: Deposition at a higher rate due to increased plasma power or increased argon partial pressure may reduce film quality.

1.2.4. Remove the wafer and repeat steps 1.2.1–1.2.3 for the second side of the wafer.

1.3. Dicing

1.3.1. Use a dicing saw to dice the entire wafer as needed.

NOTE: A protective resist can be applied on the substrate prior to dicing, and the system (**Table of Materials**) used here applies a UV curable film just before the samples are loaded on the dicing stage. It is found that dicing the samples with an automated dicing saw does not compromise the integrity of the samples. Hand-scribe dicing of LN is possible, though tedious and prone to inconsistencies.

2. Making electrical and mechanical contact with the transducer

NOTE: Several methods are described below (steps 2.1–2.4), and it is highlighted later in the protocol which method is most appropriate for each subsequent step.

2.1. Place a diced transducer flat on a magnetic steel plate. Mount one pogo-probe in contact with the plate and another pogo-probe in contact with the top surface of the transducer. Hereafter this will be referred to as pogo-plate contact.

2.2. Place the transducer between two pogo-probes. Hereafter referred to as pogo-pogo contact.

2.3. Solder wire to each face of the transducer. Hereafter referred to as solder contact.

2.4. Assemble a custom transducer holder.

2.4.1. Order the custom printed circuit boards (PCBs) whose Gerber files have been provided.

2.4.2. Solder two surface mount spring contacts (**Table of Materials**) to each custom PCB. Press

fit the spikes into the plated holes on the custom PCBs such that they point away from each other.

2.4.3. Connect the two custom PCBs with board spacers and screws so that the contacts are just in contact with each other. Adjust the spacing with plastic washers if necessary.

2.4.4. Slide a 3 mm x 10 mm transducer in between the inner pair of contacts. Clip the outer contacts so they do not short the circuit.

NOTE: **Figure 1** shows the entire assembly.

3. Resonance frequency identification via impedance analysis

3.1. Ensure that a port calibration has been performed according to the manufacturer's instructions for the specific contact method being used.

3.2. Connect a transducer to the open port of the network analyzer (**Table of Materials**) with one of the contact methods described in steps 2.1–2.4.

NOTE: It can be instructive to repeat this analysis with multiple electrical contact methods and compare the results.

3.3. Select the reflection coefficient parameter, s_{11} , via the user interface of the network analyzer, choose the frequency range of interest, and perform the frequency sweep.

NOTE: s_{11} is the input reflection coefficient and has a minimum value at the resonance frequency of operation. For a typical 500 μm thick 128YX LN wafer, the primary resonance frequency will be near 7 MHz and the second harmonic will be near 21 MHz, as illustrated in **Figure 2**. The impedance plot in frequency space displayed on the instrument will exhibit local minima at the resonance frequencies.

3.4. Export the data by selecting **Save/Recall | Save Trace Data** on the user interface for closer inspection using data processing software to identify the precise minima locations.

4. Vibration characterization via LDV

4.1. Place a transducer in pogo-plate contact on the LDV stage. Connect the pogo-probe leads to the signal generator. Ensure that the correct objective is selected in the acquisition software (**Table of Materials**) and focus the microscope on the surface of the transducer.

4.2. Define the scan points by selecting **Define scan points** or proceed to step 4.3 if performing a continuous scan.

4.3. Select the **Settings** option and under the **General** tab, select either the **FFT** or **Time** option

depending on whether the scan is being performed in frequency or time domain. Select the number of averages in this section.

NOTE: The number of averages affects scan time. Five averages for the transducers described in this protocol have shown to give sufficient signal/noise ratio.

4.4. In the **Channel** tab, make sure that the **Active** boxes are checked, which correspond to the reference and reflected signal from the transducer. Adjust the reference and incident channels by selecting a voltage value from the drop-down menu in order to obtain maximum signal strength from the substrate.

4.5. In the **Generator** tab, if the measurement is carried out under single frequency signal, select **Sine** from the **Waveform** pull down list; if it is under a band signal, select **MultiCarrierCW**.

4.6. Change the bandwidth and FFT lines in the **Frequency** tab to adjust the scan resolution for a frequency domain scan. Similarly, change the **Sample Frequency** in the **Time** tab when performing time domain measurements.

NOTE: The bandwidth typically used is 40 MHz and the number of FFT lines is 32,000. The presentation software (**Table of Materials**) can be used to process and analyze the data obtained from the scan. A typical displacement spectrum is provided in **Figure 3**.

5. Fluid supply

5.1. Obtain a 25 mm long, 1 mm diameter wick composed of a bundle of fibers of a hydrophilic polymer designed to transport aqueous liquid across its length such as those available for plug-in air fresheners.

5.2. Insert the wick into a syringe tip with an inner diameter that provides a snug fit and a length that allows the wick to extend 1–2 mm beyond each end. Lock the tip onto a syringe with the desired capacity (1–10 mL).

5.3. Mount the wick/syringe assembly such that the wick is 10°–90° from horizontal (depending on the desired atomization rate, which also depends on the applied voltage) and the tip of the wick is just in contact with the edge of the transducer as shown in **Figure 1C**.

5.4. Fill the syringe with water and apply a continuous voltage signal (starting with 20 Vpp) at the resonance frequency determined using the impedance analyzer. Adjust the voltage level until the liquid is atomized continuously without the device flooding or drying out.

6. Dynamics observation via high-speed imaging

6.1. Rigidly mount a high-speed camera horizontally on an optical table, place a transducer in

either pogo-pogo contact or pogo-plate contact on an x-y-z stage near the focal length of the camera, and position a diffuse light source at least one focal length on the opposite side of the transducer from the camera.

6.2. For pogo-pogo contact, position the fluid supply so that it does not block the camera view or the light source. For pogo-plate contact, apply fluid directly to the substrate with a pipette.

6.3. Adjust the camera focus and the x-y-z position to bring the fluid sample into sharp focus.

6.4. Estimate the frequency of the specific phenomenon to be studied based on literature. Choose a frame rate at least twice as large as this frequency according to the Nyquist rate in order to avoid aliasing.

NOTE: For example, consider capillary waves that occur on a sessile drop at a range of frequencies. Cameras limited in spatial resolution can only distinguish waves with a minimum amplitude. In this case the minimum amplitude occurs around 4 kHz so a frame rate of 8,000 frames per second (fps) is chosen.

6.5. Adjust the light intensity, the camera shutter, or both in order to optimize contrast between the fluid and the background.

NOTE: An opaque dye can be added to the fluid in order to increase the contrast.

6.6. Connect alligator clips from the amplified signal generator to the pogo-probes leads.

6.7. Capture video in the camera software simultaneously with actuation via the voltage signal either by manually triggering both at the same time or by connecting a trigger output from the signal generator to the camera.

NOTE: The typical frame rate used is 8,000 fps and a CF4 objective is used.

6.8. Save only the frames containing the phenomenon to avoid wasted storage, which is particularly relevant at large frame rates, to produce a result as shown in **Figure 4**.

NOTE: Make sure to save the file in a format that is compatible with the image processing software of choice so that useful data can be extracted.

7. Droplet size measurement via laser scattering analysis

7.1. The laser scattering system (**Table of Materials**) has a module that transmits the laser and one that receives the scattered laser signal. Position the modules along the rail provided with the system, with a 20–25 cm gap between them.

7.2. Rigidly mount a platform in this gap such that, when the transducer and fluid supply

assemblies are placed on it, atomized mist will be ejected into the laser beam path. Facilitate this alignment by turning on the laser beam and selecting **Tools | Laser Control... | Laser on** as a visual indicator.

7.3. Fix the transducer holder to the platform and fix the fluid supply assembly to an articulated arm (**Table of Materials**). Position the fluid supply assembly so that the tip of the wick is just in contact with the edge of the transducer.

7.4. Create a standard operating procedure (SOP) in the software by clicking the **New SOP** icon. Configure the SOP with the following settings: **template = Default continuous, sampling period (s) = 0.1**, under **Data handling**, click **Edit...** and set **Spray profile | Path length (mm)** to **20.0**, click **Alarms** to uncheck **Use default values** and set **Min transmission (%)** to **5** and **1** and set **Min scattering** to **50** and **10**. Leave all other settings as defaults.

NOTE: Consult the software manual that came with the instrument.

7.5. Start the measurement within the software by clicking **Measure | Start SOP** and selecting the SOP created in step 7.4 and following the onscreen guidelines. Fill the fluid supply reservoir, the syringe, with water up to the desired level and note the volume. Turn on the voltage signal to begin atomizing the fluid after the measurement has started and start the stopwatch.

7.6. The software generates a size distribution based on the scattered laser signal at the receiver due to Mie theory and a multiple scattering algorithm. Once the desired volume of fluid has been atomized, turn off the voltage signal, stop the stopwatch, and record the final volume.

NOTE: The laser scattering system is capable of measuring as little as 1 μL of fluid and does not have an upper limit for fluid volume. The atomization flow rate can simply be calculated by dividing the volume by the time duration.

7.7. In the measurement histogram, select the portion of the data during which the atomization was occurring as expected and the signal at the receiver was strong enough to be statistically significant.

NOTE: All measurements with this technique are statistical averages and thus, if there are too few droplets, then the scattered signal will be weak, and the measurement will be statistically insignificant.

7.8. Click **Average | Ok** to generate a distribution based on the selected data. Save this by selecting the window and clicking **Edit | Copy text** then pasting the result in a text file and saving with an appropriate name.

NOTE: This distribution data can now be used with other software (e.g., MATLAB) to create the plot in **Figure 5**.

REPRESENTATIVE RESULTS:

Thickness mode piezoelectric devices were fabricated from 128YX lithium niobate. **Figure 1** shows a complete assembly to hold the transducer in place with a custom transducer holder used with the passive fluid delivery system developed for continuous atomization. The characterization steps for these devices include determination of the resonant frequency and harmonics using an impedance analyzer (**Figure 2**). The fundamental frequency of the devices was found to be close to 7 MHz using the technique described in this protocol, as predicted by the thickness of the substrate. Further characterization of substrate vibration was performed using noncontact laser Doppler vibrometer measurements. These measurements determine the magnitude of displacement of the substrate and is usually in the nm range (**Figure 3**). Continuous atomization is essential to enable practical applications of thickness mode devices, and this has been demonstrated by developing a passive fluid delivery system to the substrate. Finally, two techniques were described to observe droplet vibration and atomization dynamics by performing high-speed imaging and by measuring droplet size distribution as shown in **Figure 4** and **Figure 5**.

FIGURE AND TABLE LEGENDS:

Figure 1: The whole assembly of a custom transducer holder. (A) The positions of the transducer holder and the fluid supply assembly are each controlled with articulating arms such that the tip of the wick is just in contact with the edge of the transducer. Inset (B) reveals nature of the electrical and mechanical contact with the transducer electrodes. Inset (C) reveals the nature of the contact between the transducer edge and the fluid wick.

Figure 2: The real s_{11} scattering parameter values measured over a range of 1–25 MHz for a 127.86° YX lithium niobate device, indicating the presence of a resonance peak at approximately 7 MHz.

Figure 3: A multi-carrier, FFT scan with 5 averages at each point was performed over 9 by 9 scan points defined in a 0.6 by 0.6 mm area in the frequency range 5–25 MHz. The reported displacement is the maximum displacement averaged over all points. The fundamental thickness mode for 0.5 mm thick LN can be seen at 7 MHz, and a weaker second harmonic is present at ~21 MHz. Notice there are multiple narrow peaks at each resonance due to interference with lateral modes. Multi-carrier scans spread the voltage input, so the displacement here is not an accurate measure of the performance of the device. For such a measurement, it is recommended to perform a single-frequency scan at the resonance frequency and with application relevant voltages. For example, this 10 mm x 5 mm thickness mode transducer produces a 5 nm max amplitude at 45 Vpp when driven at 6.93 MHz.

Figure 4: Onset of capillary waves on a 2 μ L water drop is indicated by an 8,000 fps video of the fluid interface; the drop is driven by a thickness mode transducer driven at 6.9 MHz, showing the significant time difference between the hydrodynamic response and the acoustic excitation.

Figure 5: Droplet size distribution is typically measured as a volume fraction versus the

droplet diameter, here comparing (A) a commercial nebulizer and (B) an LN thickness mode device, both using water.

Supplemental Figure 1: A comparison of the impedance analysis spectra for the same transducer with two different forms of electrical contact (pogo-plate, pogo-pogo, and transducer holder) shows significant differences in s_{11} scattering parameter values.

Movie 1: LDV vibration mode of 5 mm x 5 mm square transducer.

Movie 2: LDV vibration modes of 3 mm x 10 mm transducer. These are close approximations to thickness modes without the presence of significant lateral modes.

DISCUSSION:

The dimensions and aspect ratio of a transducer affects the vibration modes it produces. Because the lateral dimensions are finite, there are always lateral modes in addition to the desired thickness modes. The above LDV methods can be used to determine dominant modes in the desired frequency range for a given transducer. A square with dimensions below 10 mm typically gives a close approximation to a thickness mode. Three by ten millimeter rectangles also work well. **Movie 1** and **Movie 2** show LDV area scans of the square and the 3 mm x 10 mm transducers indicating that they are close to the thickness mode. These have been empirically determined rather than selected by simulation and design, though such methods could be used to find ideal lateral dimensions.

The method of electrical and mechanical contact with the transducer also affects the vibrations it produces since these are the boundary conditions to which the piezoelectric plate is subject. We have included an impedance spectrum for three measurement techniques: pogo-plate, pogo-pogo, and transducer holder as a comparison in **Supplemental Figure 1**. Clearly, the resonance peak locations are not changed in this case by our choices of contact. We do note that mechanical contact between the transducer and a plate surface dampens vibrations making atomization less efficient. Pogo-plate contact is used in the case of LDV measurements, because it is the simplest way to get a flat, stationary surface on which to focus the laser.

The fluid supply assembly described here relies on capillary action and gravity to passively resupply the transducer with a thin film of water as it is atomized away. The vibration of the transducer produces an acoustowetting effect that can be enough to create a thin film and avoid flooding, but in some cases a hydrophilic treatment will be necessary on the transducer surface. If continuous atomization is not achieved, this is the most likely route to resolving the problem.

Measurements were performed with an ultra-high frequency vibrometer (**Table of Materials**) here, but other LDVs may be used. Electrical contact can be made by soldering a wire to each face of the transducer, though the solder can significantly alter the resonance frequencies and modes of the transducer. Another technique is to place the transducer on a metal base and use “pogo” spring contact probes pressed into contact on the top face of the piezoelectric transducer element while it sits flat upon the stage, useful when a large area has to be scanned.

Accurate measurement of the resonance frequencies is important to efficiently operate the transducer and maximize energy throughput to mechanical motion at these frequencies. A frequency scan using the LDV provides this information, but requires a long time, on the order of tens of min. An impedance analyzer can determine the resonance frequencies much more quickly, often less than a minute. However, unlike the LDV, the impedance-based measurement does not provide information on the vibration amplitude at the resonance frequencies, which is important in determining fluid atomization off the surface of the transducer.

Though vibration of the substrate occurs in the 10–100 MHz regime, the dynamics of fluids in contact with the substrate occur at far slower time scales. For example, capillary waves on the surface of a sessile drop are observable at 8,000 fps, assuming that the spatial resolution of the camera can distinguish the amplitude of a wave crest and that the wave frequency of interest is below 2,000 Hz. The camera arrangement described above images transmitted light and thus is good for observing the outline of objects that transmit light differently than air. If insufficient, a reflected or fluorescent light arrangement may be required. The exposure time for each frame decreases as the frame rate is increased so the light intensity must be increased accordingly. The objective lens should be chosen based on the length scale of the phenomenon under study, but the above protocol will work with any commonly available magnification. As an example, **Figure 4** was obtained with the above high-speed video method. The contrast at the drop interface would allow these frames to be segmented in software (ImageJ and MATLAB) so that the interface dynamics may be tracked over time.

In the droplet sizing equipment used in this protocol (**Table of Materials**), the laser optics and scattering detectors are relatively standard but the software is proprietary and complex. In addition to Mie theory, multiple scattering events make droplet size and enumeration calculations much more difficult. Mie theory assumes that most photons are scattered only one time, but when droplets are densely spaced, i.e., the spacing between droplets is not much larger than the droplets themselves, and the spray plum covers a sufficiently large area, then this assumption fails¹⁸. As an example of troubleshooting results from this instrument, consider **Figure 5**. Notice that the 0.5 mm diameter peak appears in both distributions. The commercial nebulizer is known to produce monodisperse droplets near 10 μm , so the larger peak is likely either a false result due to the large amount of multi-scattering events or agglomeration of smaller droplets within the spray. This implies that the large peak in the thickness mode distribution may also be a false result. This can be directly verified by high-speed video: such large droplets would be readily visible, but they are not observed in this case.

Laser scattering particle size analysis can also be difficult when the scattering signal becomes weak. This is typically due to a low atomization rate or when part of the spray does not pass through the laser path. A weak vacuum may be used to draw the complete atomized mist through the expanded laser beam of the equipment in cases where it would otherwise escape measurement. For even greater control of spray conditions a humidity chamber can be installed around the laser beam path, but this is not required.

ACKNOWLEDGMENTS:

The authors are grateful to the University of California and the NANO3 facility at UC San Diego for provision of funds and facilities in support of this work. This work was performed in part at the San Diego Nanotechnology Infrastructure (SDNI) of UCSD, a member of the National Nanotechnology Coordinated Infrastructure, which is supported by the National Science Foundation (Grant ECCS-1542148). The work presented here was generously supported by a research grant from the W.M. Keck Foundation. The authors are also grateful for the support of this work by the Office of Naval Research (via Grant 12368098).

DISCLOSURES:

The authors have nothing to disclose.

REFERENCES:

1. Wood, R.W., Loomis, A.L. XXXVIII.physical and biological effects of high-frequency sound-waves of great intensity. *The London, Edinburgh, and Dublin Philosophical Magazine and Journal of Science*. **4** (22), 417–436 (1927).
2. Dalmoro, A., Barba, A.A., Lambert, G., d’Amore, M. Intensifying the microencapsulation process: Ultrasonic atomization as an innovative approach. *European Journal of Pharmaceutics and Biopharmaceutics*. **80** (3), 471–477 (2012).
3. Namiyama, K., Nakamura, H., Kokubo, K., Hosogai, D. Development of ultrasonic atomizer and its application to S.I. engines. *SAE Transactions*. 701–711(1989).
4. Qi, A., Yeo, L.Y., Friend, J.R. Interfacial destabilization and atomization driven by surface acoustic waves. *Physics of Fluids*. **20** (7), 074103 (2008).
5. Wang, J., Hu, H., Ye, A., Chen, J., Zhang, P. Experimental investigation of surface acoustic wave atomization. *Sensors and Actuators A: Physical*. **238**, 1–7 (2016).
6. James, A., Vukasinovic, B., Smith, M.K., Glezer, A. Vibration-induced drop atomization and bursting. *Journal of Fluid Mechanics*. **476**, 1–28(2003).
7. Randall, C.A., Kim, N., Kucera, J.P., Cao, W., Shrout, T.R. Intrinsic and extrinsic size effects in fine-grained morphotropic-phase-boundary lead zirconate titanate ceramics. *Journal of the American Ceramic Society*. **81** (3), 677–688 (1998).
8. Tsai, S.C., Lin, S.K., Mao, R.W., Tsai, C.S. Ejection of uniform micrometer-sized droplets from Faraday waves on a millimeter-sized water drop. *Physical Review Letters*. **108** (15), 154501 (2012).
9. Jeng, Y.R., Su, C.C., Feng, G.H., Peng, Y.Y., Chien, G.P. A PZT-driven atomizer based on a vibrating flexible membrane and a micro-machined trumpet-shaped nozzle array. *Microsystem Technologies*. **15** (6), 865–873 (2009).
10. Lupascu, D., Rödel, J. Fatigue in bulk lead zirconate titanate actuator materials. *Advanced Engineering Materials*. **7** (10), 882–898 (2005).
11. Kawamata, A., Hosaka, H., Morita, T. Non-hysteresis and perfect linear piezoelectric performance of a multilayered lithium niobate actuator. *Sensors and Actuators A: Physical*. **135** (2), 782–786 (2007).
12. Qi, A., Yeo, L., Friend, J., Ho, J. The Extraction of Liquid, Protein Molecules and Yeast Cells from Paper Through Surface Acoustic Wave Atomization. *Lab on a Chip*. **10** (4), 470–476 (2010).
13. Collignon, S., Manor, O., Friend, J. Improving and Predicting Fluid Atomization via Hysteresis-Free Thickness Vibration of Lithium Niobate. *Advanced Functional Materials*. **28** (8),

526 1704359 (2018).
527 14. Lawson, A. The vibration of piezoelectric plates. *Physical Review*. **62** (1–2), 71 (1942).
528 15. Fukushima, Y., Nishizawa, O., Sato, H. A performance study of a laser doppler vibrometer for
529 measuring waveforms from piezoelectric transducers. *IEEE Transactions on Ultrasonics,*
530 *Ferroelectrics, and Frequency Control*. **56** (7), 1442–1450 (2009).
531 16. Thoroddsen, S., Etoh, T., Takehara, K. High-speed imaging of drops and bubbles. *Annual*
532 *Reviews in Fluid Mechanics*. **40**, 257–285 (2008).
533 17. Yule, A., Al-Suleimani, Y. On droplet formation from capillary waves on a vibrating surface.
534 *Proceedings of the Royal Society of London Series A: Mathematical, Physical and Engineering*
535 *Sciences*. **456** (1997), 1069–1085 (2000).
536 18. Hirleman, E.D. Modeling of multiple scattering effects in Fraunhofer diffraction particle size
537 analysis. In *Optical Particle Sizing*. Edited by Gouesbet, G., Gréhan, G., 159–175, Springer.
538 Boston, MA (1988).

Fig 1

[Click here to access/download/Figure;Figure1.eps](#)

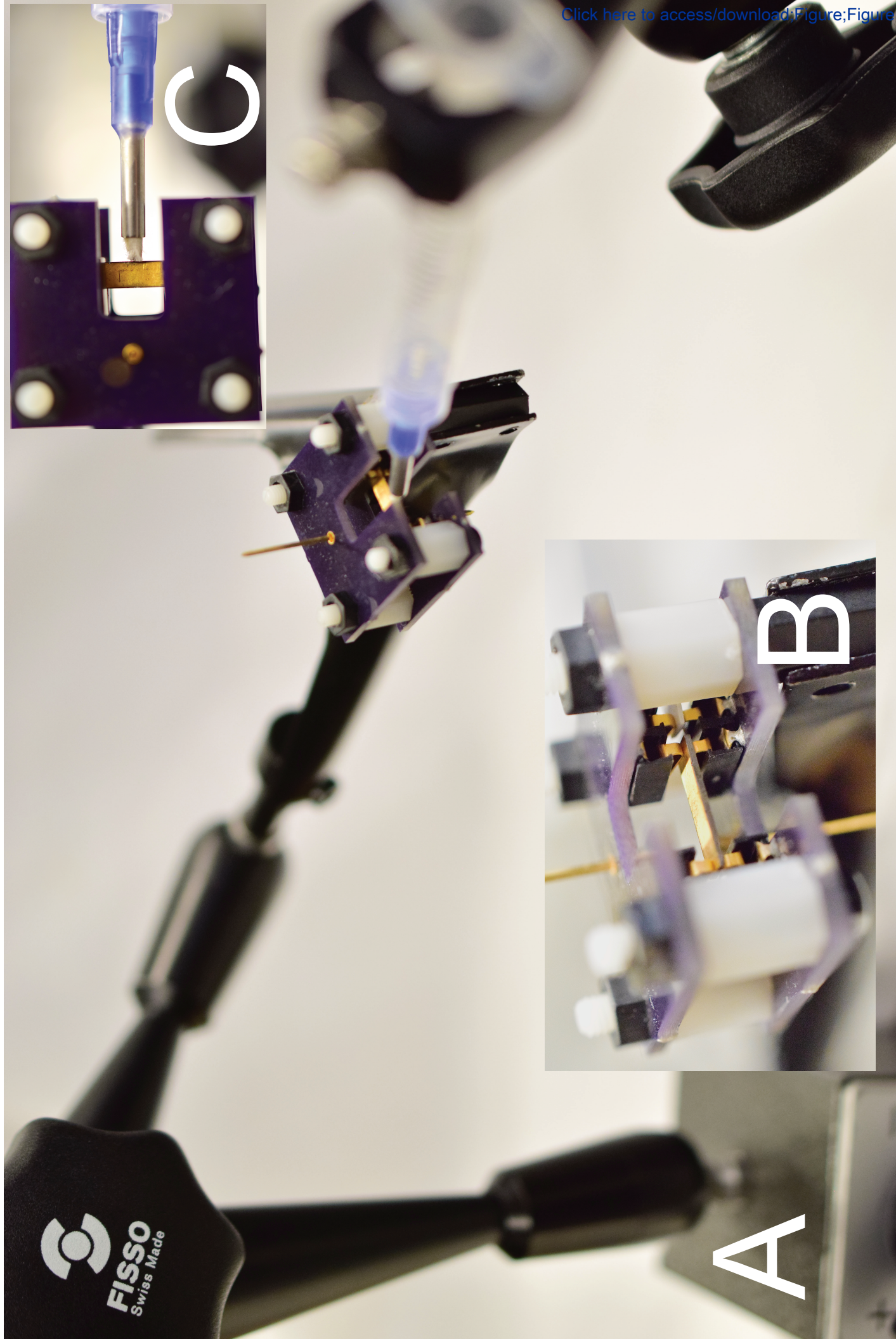


Fig 2

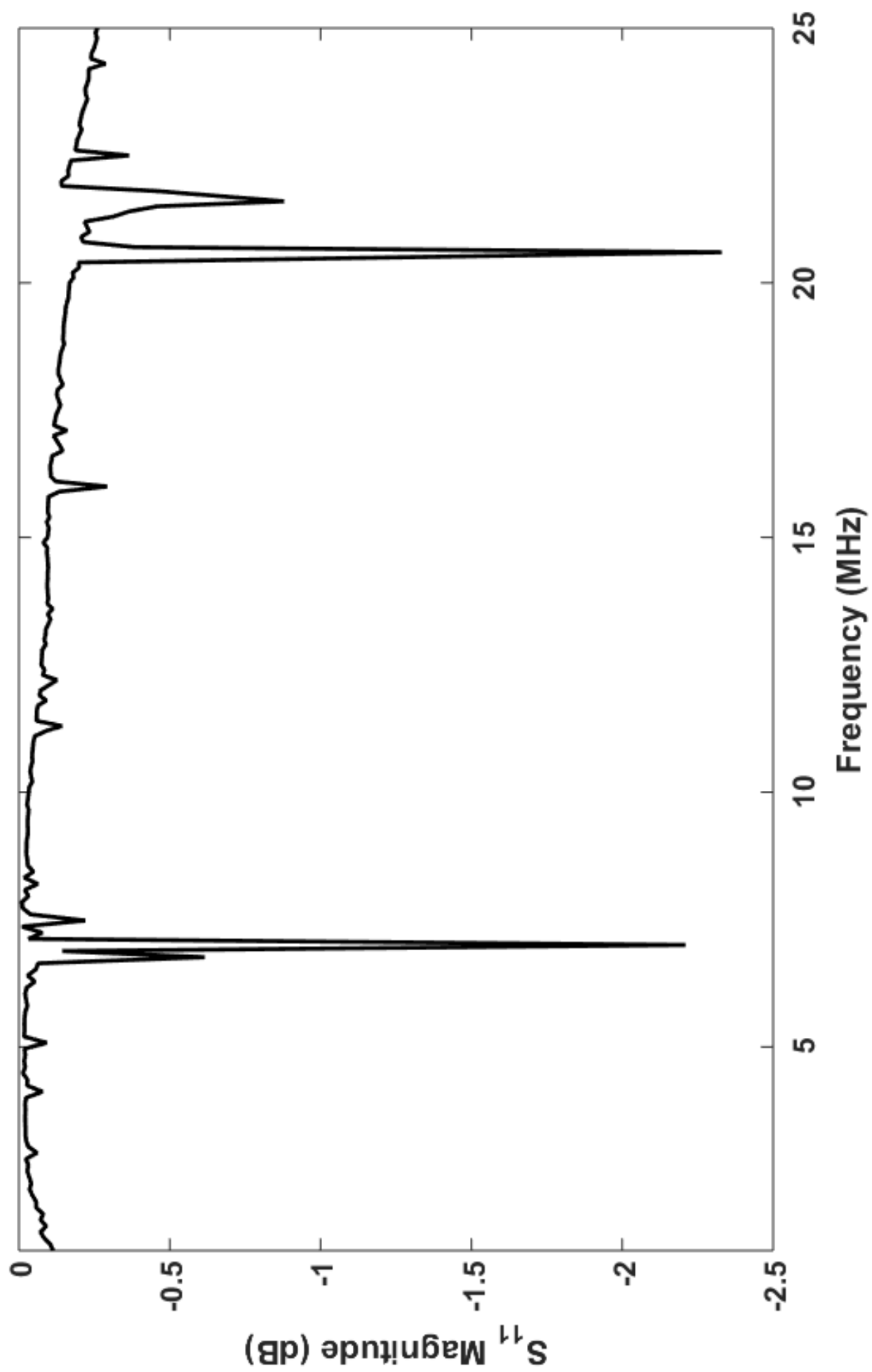
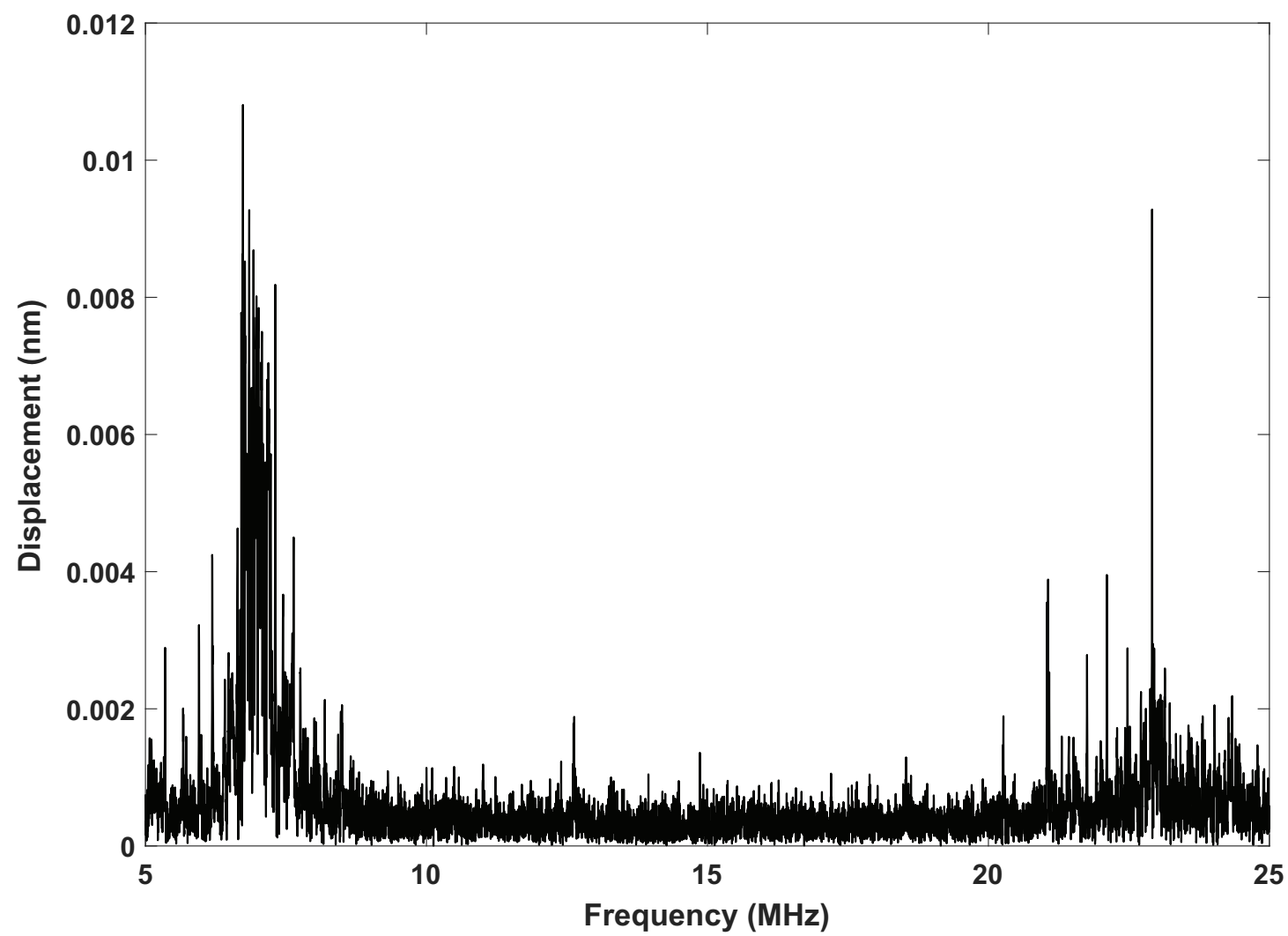


Fig 3



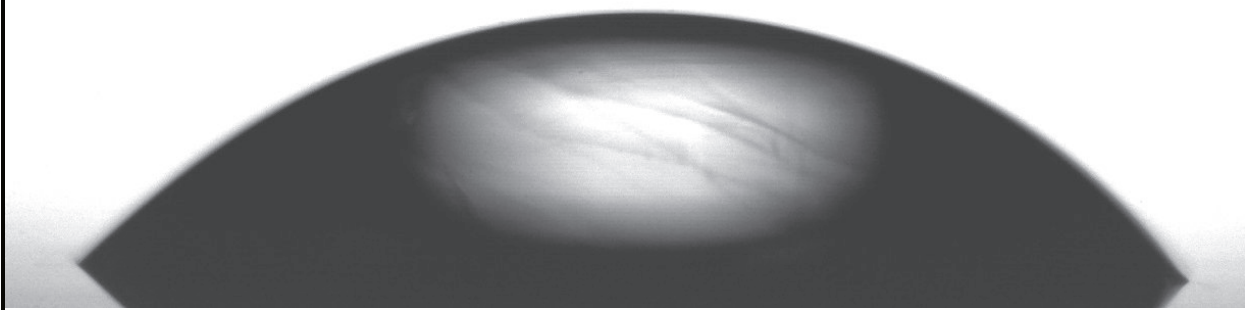
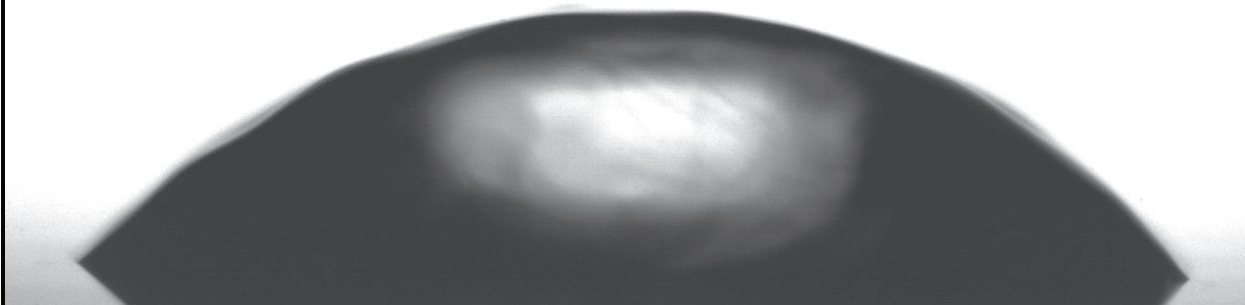
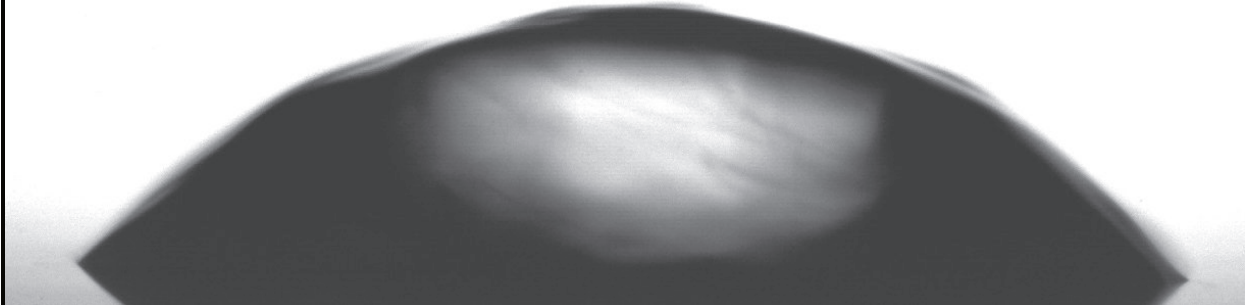
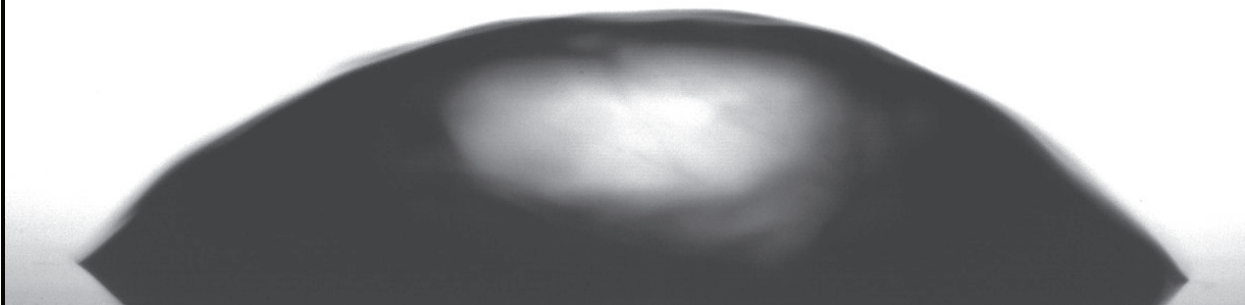
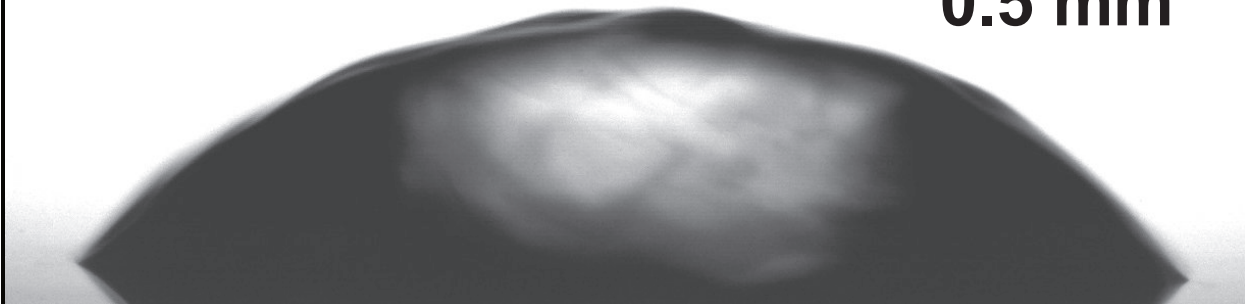
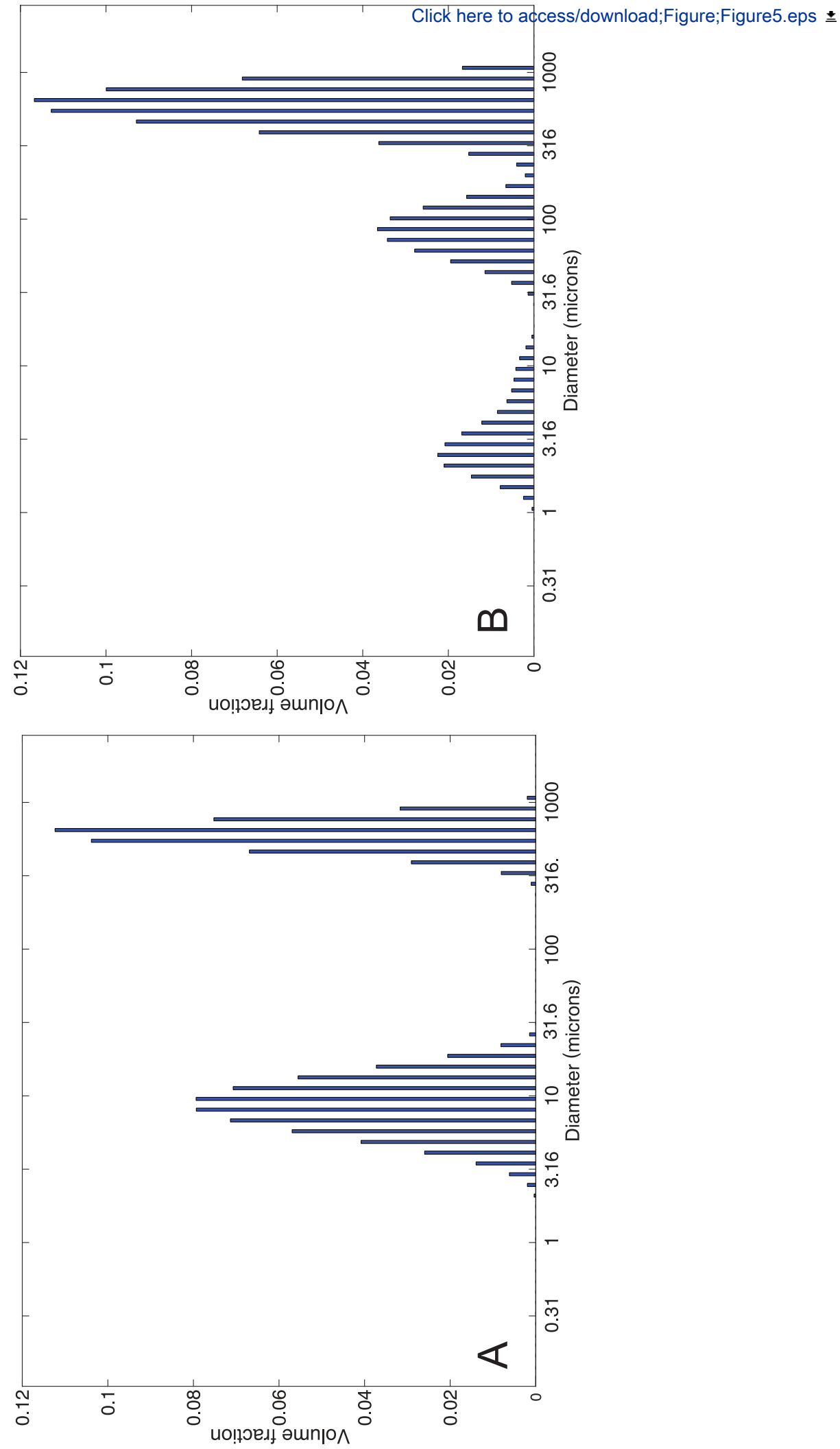
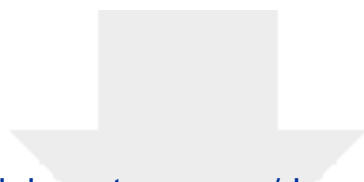
0 ms**100 ms****200 ms****300 ms****400 ms**
0.5 mm

Fig 5

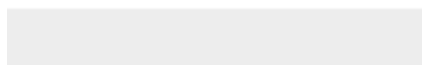
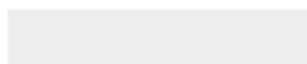




[Click here to access/download](#)

Video or Animated Figure

Movie1-TMscan5x5_Nov2018_1_6.6371875_MHz.avi

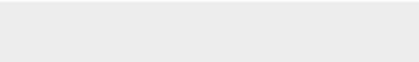
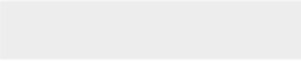




Click here to access/download

Video or Animated Figure

Movie2-TMscan10x3(5-8MHz,
0,15Vx5Wamp)_6.450625_MHz.avi



Name of Material/Equipment	Company
Amplifier	Amplifier Research, Souderton, PA, USA
Articulating arm	Fisso, Zurich, Switzerland
CF4 Objective	Edmund Optics, Barrington, NJ, USA
Dicing saw	Disco, Tokyo, Japan
Fiber Fragrance Diffuser Wick	Weihai Industry Co., Ltd., Weihai, Shandong, China
High Speed Camera	Photron, San Diego, USA
Laser Doppler Vibrometer	Polytec, Waldbronn, Germany
Laser Scattering Droplet size measurement system	Malvern Panalytical, Malvern, UK
Lithium niobate substrate	PMOptics, Burlington, MA, USA
Luer-lock syringes	Becton Dickinson, New Jersey, USA
Nano3 cleanroom facility	UCSD, La Jolla, CA, USA
Network Analyzer	Keysight Technologies, Santa Rosa, CA, USA
Oscilloscope	Keysight Technologies, Santa Rosa, CA, USA
PSV Acquisition Software	Polytec, Waldbronn, Germany
PSV Presentation Software	Polytec, Waldbronn, Germany
Signal generator	NF Corporation, Yokohama, Japan
Single Post Connector	DigiKey, Thief River Falls, MN
Sputter deposition	Denton Vacuum, NJ, USA
Surface Mount Spring Contacts	DigiKey, Thief River Falls, MN
Teflon wafer dipper	ShapeMaster, Ogden, IL, USA
XYZ Stage	Thor Labs, Newton, New Jersey, USA

Catalog Number

5U1000

Disco Automatic Dicing Saw 3220

https://www.weihaiz.com/Fiber-Fragrance-Diffuser-Wick_p216.htm

Fastcam Mini

UHF120

STP5315

PWLN-431232

5061B

InfiniiVision 2000 X-Series

Version 9.4

Version 9.4

WF1967 multifunction generator

ED1179-ND

Denton 18

70AAJ-2-MOGCT-ND

SM4WD1

MT3

Comments/Description

Objective used for high speed imaging

[nl](#)

Non-contact laser doppler vibrometer

4" double-side polished 0.5 mm thick 128°Y-rotated cut lithium niobate

Fabrication process is performed in it.

LDV Software

LDV Software

Denton Discovery 18 Sputter System

Wafer Dipper 4"

Optical table stages

After revising and uploading your submission, please also upload a separate rebuttal document that addresses each of the editorial and peer review comments individually. Please submit each figure as a vector image file to ensure high resolution throughout production: (.psd, ai, .eps., .svg). Please ensure that the image is 1920 x 1080 pixels or 300 dpi. Additionally, please upload tables as .xlsx files.

The figures and table have been submitted per JoVE format recommendations.

Editorial comments:

Changes to be made by the author(s) regarding the manuscript:

1. Please take this opportunity to thoroughly proofread the manuscript to ensure that there are no spelling or grammar issues. The JoVE editor will not copy-edit your manuscript and any errors in the submitted revision may be present in the published version.

The manuscript has been reviewed for spelling and grammar issues.

2. Please number the figures in the sequence in which you refer to them in the manuscript text.

The figure numbering has been updated.

3. References: Please use the JoVE EndNote style file and ensure that the references appear as the following: [Lastname, F.I., LastName, F.I., LastName, F.I. Article Title. Source. Volume (Issue), FirstPage – LastPage (YEAR).] For more than 6 authors, list only the first author then et al. Please do not abbreviate journal titles. See the example below:

Bedford, C.D., Harris, R.N., Howd, R.A., Goff, D.A., Koolpe, G.A. Quaternary salts of 2-[(hydroxyimino)methyl]imidazole. Journal of Medicinal Chemistry. 32 (2), 493-503 (1998).

The references have been updated per JoVE guidelines.

Reviewers' comments:

Reviewer #1:

Manuscript Summary:

I'd like to thank the authors for including almost all suggested changes. The manuscript, especially the technological protocol benefits from this.

Minor Concerns:

There are few comments from my side:

-In the revised version, Figure 2 still lacks important information, i.e. axes with description and information on the boundary condition of the measurement.

The caption for figure 2 has been updated with more information regarding the measurement.

-Line 24-26: Please provide evidence, of the higher efficiency of these devices "in terms of flow rate per power input, than those that rely on Rayleigh waves and other modes of vibration in LN or PZT", taking account a well comparable droplet size distribution. If no evidence is provided, I suggest to soften the statement to "Such devices may be able to atomize liquid more efficiently..."

The evidence for this claim—notably the figure of merit and data that indicate a substantially greater atomization flow for a given input power—is detailed in the publication cited in the second paragraph of the introduction, where we make the same claim as in the abstract. We cannot include the citation in the abstract but have provided it in the introduction and have included it below for the reviewer's consideration.

Collignon, Sean, Ofer Manor, and James Friend. "Improving and Predicting Fluid Atomization via Hysteresis-Free Thickness Vibration of Lithium Niobate." Advanced Functional Materials 28.8 (2018): 1704359.

Reviewer #2:

The authors have made comprehensive alterations to the manuscript which adequately address all the points I raised in the initial review. I think this is a useful and well described protocol and ready for publication.

We are grateful to the reviewer for their comments and questions for the previous version, as this version is much improved as a consequence.

Reviewer #3:

Manuscript Summary:

The subject of the manuscript is interesting, however the title and the abstract cant inform to the reader the real scope of the work.

Major Concerns:

- a) Change the title. use una more indicative of the scope. You are constructing and characterising a ultrasonic atomization system.. not a thickness mode transducer
- b) The same for the summary and the abstract

The example is an atomizer, but the process of fabrication and testing, altogether four of the five steps, describe the work to fabricate and characterize a thickness-mode transducer. The atomizer is one of many possible applications of this simple structure, and the point of the

protocol is to fabricate and characterize the resonator devices for this broader range of acoustofluidic applications. Atomization is just one of them, a convenient example for our purposes. Thus the title, summary, and abstract as provided. However, our introduction begins and finishes with a discussion of atomization, and so we have added “Atomization and Acoustofluidics” to the title in recognition of this concern.

Minor Concerns:

c) Why don't you buy the crystals with electrodes?

They're not commercially available except in very large batch quantities. Lead zirconate transducers are widely available, but these are not single crystal and quite inefficient by comparison.

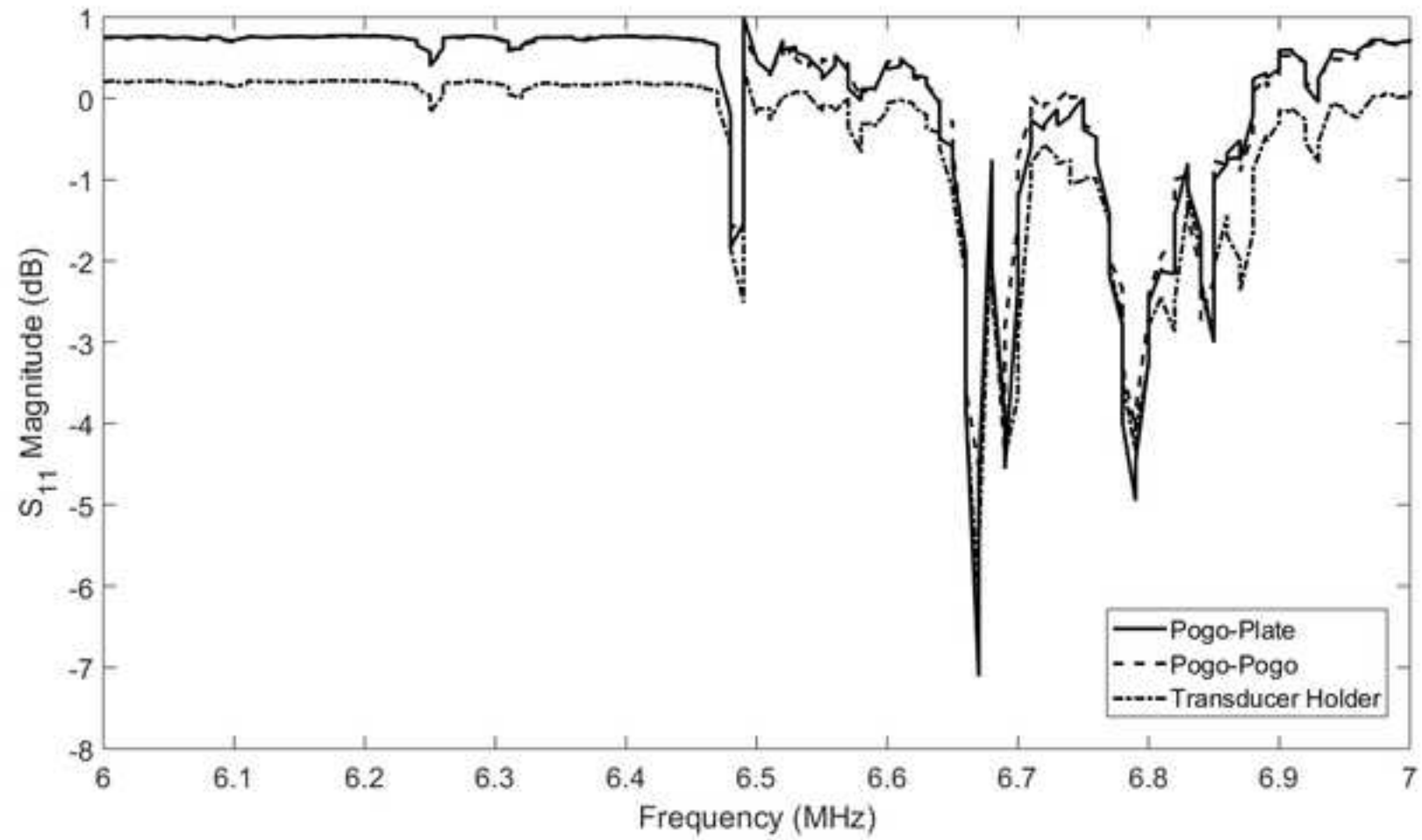
Further, the electrode thickness and quality directly affect the transducer efficiency for acoustofluidics. We have developed and characterized these parameters in order to lower power consumption by the device for the specific case during atomization.

d) delete the comment about the high speed camera. You can only declare the procedure used by you...

We're unsure what this is referring to, as the text describing the use of high speed cameras is present in several locations in the manuscript. In fact, high-speed imaging is crucial to understanding most acoustofluidic phenomena, whether by us or by a prospective reader, and in making this point we have added a brief statement to the text on line 69, “In atomization, like many other acoustofluidic phenomena,...”

c) the text in line 75 is very descriptive. I suggest to include in the abstract or in the summary

We have revised the abstract slightly to highlight the point that fluid control is important in atomization.





Click here to access/download
Supplemental Coding Files
TM_Holder_Gerbers.zip